Identifying oceanographic conditions conducive to coastal impacts on temperate open coastal beaches and the importance of empirical impact data

Chloe Leach (chloe.leach@unimelb.edu.au)
The University of Melbourne https://orcid.org/0000-0002-3335-5620
Ben S. Hague
Australian Bureau of Meteorology
David M. Kennedy
The University of Melbourne
Rafael C. Carvalho
Deakin University
Daniel Ierodiaconou
Deakin University

Research Article

Keywords: Coastal Impacts, waves, sea level, coastal change, coastal erosion

Posted Date: March 3rd, 2021

DOI: https://doi.org/10.21203/rs.3.rs-272918/v1

Abstract

Warnings issued by meteorological or oceanographic agencies are a common means of allowing people to prepare for likely impactful events. Quantifying the relationships between ocean conditions and coastal impacts is crucial for developing operational coastal hazard warnings. Existing studies have largely omitted empirical data, relying on modelling to estimate total water levels and impact potentials. It is well documented that site-specific conditions influence local morphodynamics and as such, detailed data related to the physical environment is a necessary component of these existing approaches. The capacity to collect this data is not always available and there is a need for the inclusion of physical impact events to properly quantify the effects of natural hazards and identify the conditions that they are likely to occur.

We propose an alternative empirically-based framework for isolating oceanic conditions that are conducive to impact along open coasts, using two case studies from Victoria, southeast Australia: Port Fairy and Inverloch. Oceanic conditions were defined using data obtained from a WAVEWATCH III (WW3) model hindcast, assessed against newly-installed wave buoys, which evidenced variation in mean conditions between the two sites. We coupled impact-based data derived from citizen-science and social media to modelled and observational data, to identify the oceanic conditions that led to these impacts. We found heterogeneity in the response of the case study locations to deviations from the local mean wave characteristics and still water levels. This paper demonstrates a framework through which impact-based thresholds for erosion could be developed for management applications and early-warning systems.

1 Introduction

The impacts of climate change in coastal areas, such as increased erosion and inundation, are commonly attributed to the effects of mean sea-level rise, with an increasing focus on how extreme sea levels (ESLs) will change in the future (Church et al. 2006; O'Grady et al. 2019a). ESLs can be defined according to their probability of occurrence (e.g. McInnes et al. 2016; O'Grady et al. 2019a; Meucci et al. 2020; Kirezci et al. 2020) or their impact (e.g. Hague et al. 2019, 2020), with both approaches giving unique insights into the spatial and temporal scales of events. Climate change is likely to change ESL drivers, which, particularly in concurrence with rising mean sea level, will result in an increase in adverse/damaging coastal impacts (Church et al. 2006). Studies have further shown that the height of ESLs could increase further than that which will occur due to global mean sea level (GMSL) rise in some locations (Pickering et al. 2017; Devlin et al. 2017; Harker et al. 2019; Muis et al. 2020; Meucci et al. 2020). For example, research has noted the importance of understanding the contribution of storms (Stephens et al. 2020), astronomical tides (Hague et al. 2020) and wave climate conditions (O'Grady et al. 2019a) to the total water level and resulting coastal impacts (Church et al. 2006; Ranasinghe 2016; Hague et al. 2020). Individually, each factor may not be considered extreme but can compound to an ESL event which causes greater impact to the coast (Church et al. 2006; Hague et al. 2020).

GMSL increased at a rate of 1.7 (1.5–1.9) mm yr^{-1} between 1900–2010, increasing to 3.2 (2.8–3.6) mm yr^{-1} between 1993–2010 and 3.6 (3.1–4.1) mm yr^{-1} between 2006–2015 (Wong et al. 2015; Pörtner et al. 2019), where parenthesized values denote the 5^{th} and 95^{th} percentile trend estimates. By 2100, GMSL is projected to rise by between 0.44 (0.28–0.6) mm yr^{-1} (low emissions scenario) and 0.74 (0.52–0.98) mm yr^{-1} (high emissions scenario) (Wong et al. 2015), with similar values projected for Australian waters (McInnes et al. 2015). Whilst there is relatively low confidence in future wave climate (wave height, direction and period) projections within the IPCC (Wong et al. 2015), studies show that approximately 40% of coastlines are likely to experience changes in at least two principal

wave variables, including shifts in wave height and period by 5-15% and wave direction by 5-15^{o} based on a high emission scenario (Morim et al. 2019). Impacts can be magnified where rotation of the wave climate increases shoreline exposure and dampened where rotation decreases shoreline exposure (Leach et al. 2020).

Numerous studies have investigated Australian meteorological and oceanographic events and the relative contribution of different ESL physical drivers at specific locations (Mortlock et al. 2017; e.g. Harley et al. 2017). Studies have also investigated relationships between large-scale climate variability and wave heights around Australia, including the Madden-Julian Oscillation (Marshall et al. 2015), Southern Annular Mode (Hemer et al. 2010; Marshall et al. 2018) and split-flow blocking high pressure systems (Marshall et al. 2020). However, very few have quantified the physical drivers in a way that facilitates national or regional warning and monitoring for these hazards. This is likely due to significant gaps in driver and impact data (Greenslade et al. 2020) and the complexity in calculating important local scale characteristics, such as nearshore wave transformations (O'Grady et al. 2019a). This is further made complex by changes in the total water level, including GMSL and ESL, not occurring homogeneously around the world's coastlines due to variability in the natural system (Kirezci et al. 2020). The subsequent reporting of societal impact is further complicated by highly variable perceptions of coastal hazards and unstandardised reporting of these hazards (Moore and Obradovich 2020).

As sea levels continue to rise, we anticipate that erosion and flooding at known or emerging hot-spots (i.e. coastal areas where assets are located in what would otherwise be the accommodation space for shoreline recession) will worsen (e.g. Vousdoukas et al. 2020, Cooper et al. 2020), and it is likely that informed decisions will need to be made about coastal management, including planning for managed retreat. Whilst local scale variability and site-specific conditions are important in modulating coastal impacts, recent research has shown that we can identify the broader-scale oceanographic conditions that are conducive to impacts irrespective of these local conditions (Hague et al. 2019). This does not imply that these local factors, such as beach slope, short-term variability in coastal morphology and sedimentology, do not influence case-by-case impact occurrences or characteristics. More, that we can correlate impact occurrence to their broader, contemporaneous oceanographic conditions. This approach also has the advantage of not requiring local-scale data or running of mathematical model simulations for complex calculations, for example, of wave setup (O'Grady et al. 2019b), which is not always achievable due to a lack of data and resources. For example, Hague *et al.* (2019) found that coastal inundation impacts occurred across large spatial domains, driven by high astronomical tides across a large region, overwhelming the role of compartment-scale physical variability. A similar pattern is found in modelling tsunami impact in Australia (Allen and Greenslade 2016) and inundation in the Marshall Islands (Smith and Juria 2019). Defining impact-based thresholds (Hague *et al.*, 2019, 2020; Smith and Juria 2019) provides the potential for quantifying the collective effects of waves, storm surges and tides in a unified impact-based framework, even if the individual effects of these drivers are minor (McInnes et al. 2016). It would also allow for site specific warning approaches to be developed, not unlike those currently in place for riverine flooding.

In this paper, a correlative approach is used to investigate the potential to identify oceanographic conditions that lead to impacts (e.g. flooding, erosion) without the need to consider highly localized environmental factors and human influences. We use two locations on high energy temperate open coasts in Victoria, Australia which are exposed to swells generated in the Southern Ocean, as a proof-of-concept. We further highlight the importance of collecting more formal coastal impact observations, in order to develop regional impact-based coastal hazard warnings and demonstrate the potential to achieve this using the approach employed herein.

2 Study Sites

The southern coast of Australia is considered to have one of the most globally energetic wave climates (Hemer and Griffin 2010; Hughes and Heap 2010) generated from the almost continuous fetch around the Southern Ocean and strong westerly winds (Young et al. 2020). Deep-water wave conditions are spatially variable, particularly along the Victorian coastline in the southeast of Australia (Figure 1) where wave blocking from Tasmania and other islands in Bass Strait, as well as the shallow and wide continental shelf acting to reduce wave energy and limit fetch along the central part of the Victorian coast (McSweeney 2020). Tides are amplified from west to east in Bass Strait, from a tidal range of 1 m at Warrnambool to 3.3 m at Stony Point (Australian Hydrographic Service 2012). Extreme total water levels (1-in-100 year recurrence interval) are greatest between Western Port Bay and Wilsons Promontory, ranging from 3.5-4.5 m and are lower outside of Bass Strait, ranging from 2.5-3.5 m for southwesterly facing shorelines and 1.5-2.5 m for those that are southeasterly facing (O'Grady *et al.*, 2019). Port Fairy and Inverloch have been selected as field laboratories, situated on the western and central-eastern side of the Victorian coast respectively, chosen to represent differences in wave energetics along the Victorian Coast (Figure 1).

East Beach in Port Fairy is a southeasterly facing sandy coastal system on the western side of the Victorian coast, with an approximate shoreline length of 5.8 km (Figure 1). Although this stretch of coastline is exposed to some of the most energetic wave conditions along the Victorian coast (McSweeney 2020), the orientation of this embayment and wave blocking from Griffiths Island at the southern end of the beach, results in reduced wave energy here (Leach et al. 2020). East Beach in Port Fairy has been subject to erosion since the 1870s following the construction of training walls at the entrance to the Moyne River at the southern end of the embayment. It has since undergone a series of management measures including dredging of the Moyne River to maintain access after the installation of the training walls, installation of a basalt breakwater in 1910, a rock revetment in the 1950s which has been extended and altered over time and a series of timber groynes built in the 1970s (Flocard et al. 2013). Over 2 km of East Beach is protected to some extent by these structures, but unprotected areas are reportedly receding at a rate of between 0.1-0.3 m yr^{-1} (Flocard et al. 2013) and volumetric losses across the whole of East Beach have been estimated at 39 m^3 yr^{-1} between 1977 and 2007 (Carvalho et al. 2020). The erosional behavior of this system has been highly influenced by the management measures, particularly the construction of the Moyne River training walls which has reduced longshore sediment transport around Griffiths Island and into the system (Carvalho et al. 2020).

Inverloch is situated within the shadowed hook of Venus Bay, a southwesterly facing crenulate bay along the eastern coast of Victoria (Figure 1). Inverloch is sited on the northern shore of the shallow tidal estuary of Anderson inlet. It has three primary beaches, the most westerly of which (Main Beach) is outside of the mouth of the Inlet and exposed to the open ocean. The shoreline faces a southerly direction and is exposed to the dominant southwesterly waves as they refract around Cape Patterson. Shoreline change is spatially and temporally variable, with different periods and sections of coastline having recessional and accretional behaviors over the past 30 years (Doumtsis 2020; Konlechner et al. 2020). Erosion along Main Beach has been more frequently documented since 2013 and it has been estimated that approximately 40 m of recession occurred along some of the most severely impacted sections of this beach between 2013-2018 (Doumtsis 2020; South Gippsland Conservation Society Inc. 2020).

3 Methods And Data

3.1 Wave Climate

Wave climate data was sourced from the Centre for Australian Weather and Climate Research (CAWCR) WAVEWATCH III (WW3) wave hindcast (Durrant *et al.*, 2013, Smith et al. 2020); herein, referred to as WW3. This hourly dataset was generated with the WW3 model which was run at a 4-arc minute resolution around the coast of Australia for the

period 1979-2020; January 1979 is excluded from analyses herein, since it is considered a model spin-up period. There have been slight variations to the model version and input conditions over this period: 1979-2010 was generated using WW3 v4.08 forced with NCEP CFSR hourly winds and daily sea ice, 2011-May 2013 was generated using WW3 v4.08 forced with NCEP CFSv2 hourly winds and daily sea ice, and June 2013-onwards was generated using WW3 v4.18 forced with NCEP CFSv2 hourly winds and daily sea ice (Durrant *et al.*, 2013, Smith et al. 2020).

Gridded wave climate data from WW3 was averaged across 24 grid cells surrounding Port Fairy and 35 surrounding Inverloch, to appropriately sample the wave conditions, according to the different coastal geometries, settings and location of the wave buoys (Figure 1). The following integrated parameters were considered: significant wave height (H_s), mean (θ_m) and peak (θ_p) nautical wave direction, and mean (T_m) and peak (T_p) wave period. Sea state was classified based on the height of waves according to the Douglas Scale, that is expressed in Degrees (D) from 0 (no measurable waves) to 9 (phenomenal, >14 m waves) (Bureau of Meteorology 2020a).

The performance of the WW3 model in Inverloch and Port Fairy was assessed against hourly data from two SOFAR Spotter wave buoys, deployed as part of the Victorian Coastal Monitoring Program (VCMP) (VCMP 2020; Greenslade et al. 2020). The Port Fairy wave buoy is ~ 3 km offshore in ~20 m water depth and the Inverloch buoy is sited ~10 km offshore in ~50 m water depth (Figure 1). The raw buoy data was quality controlled using the Hampel Filtering process, removing outliers that exceed the median of a window of values (6) by more than three standard deviations.

WW3 data was evaluated against in-situ buoy measurements during January 2020 (Inverloch deployed 8th January 2020) using the Normalized Mean Bias Error (NMBE) (Eq. 1), Normalized Root Mean Square Error (NRMSE) (Eq. 2) and Correlation Coefficient (r) (Eq. 3):

$$\mathrm{NMBE} = \frac{1}{\bar{m}} \cdot \frac{\sum_{i=1}^{n} (s_i - m_i)}{n} \quad (1)$$

$$\mathrm{NRMSE} = \frac{1}{m^{(max-min)}} \cdot \sqrt{\frac{\sum_{i=1}^{n} (s_i - m_i)^2}{n}} \quad (2)$$

$$r_{ms} = \frac{\sum_{i=1}^{n} (m_i - \bar{m})(s_i - \bar{s})}{\sqrt{\sum_{i=1}^{n} (m_i - \bar{m})^2} \sqrt{\sum_{i=1}^{n} (s_i - \bar{s})^2}} \quad (3)$$

where n is the sample size, m is the measured buoy data and s is the simulated data.

A strong correlation was found between modelled and measured H_s at both sites, with an R value of 0.79 in Port Fairy and 0.96 in Inverloch (Table 1, Figure 2). The peak direction and peak period define conditions associated with the most energetic waves and would be considered the more appropriate metric for impact-based studies compared to the mean. However, the low correlations between modelled and measured peak data justifies the use of the mean in this instance (Table 1). A strong correlation was found between modelled and measured θ_m and T_m at both sites (Table 1).

Table 1: Model performance indices (Eq. 1-3) for WW3 outputs compared against in-situ wave data for Port Fairy and Inverloch in January 2020.

	Port Fairy					Inverloch				
	H_s (m)	θ_m (º)	θ_p (º)	T_m (s)	T_p (s)	H_s (m)	θ_m (º)	θ_p (º)	T_m (s)	T_p (s)
NMBE	0.27	0.09	0.09	0.04	0.06	0.06	0.01	0.01	-0.04	0.15
NRMSE	0.25	0.28	0.30	0.12	0.12	0.06	0.05	0.12	0.11	0.25
R	0.79	0.88	0.61	0.84	0.67	0.96	0.95	0.48	0.86	0.42

3.2 Sea Level

Sea level data from the Bureau of Meteorology (2021), with hourly tide gauge observations and residuals (i.e. predictions minus astronomical tides) from the Portland Australian Baseline Sea Level Monitoring Project (ABSLMP) tide gauge used in this analysis (Figure 1). Values of high astronomical tides (HT) were obtained by subtracting the residual value from the observed values. A changepoint detection algorithm was written in Matlab R2017b to identify the times of high tides and these values and their coincident residual values (RES) used in event impact analysis.

There are no tide gauges at Port Fairy or Inverloch, and whilst Portland is the closest gauge to Port Fairy it is further from Inverloch. The nearest gauges to Inverloch are Stony Point located approximately 50 km northwest inside Western Port Bay, and Port Welshpool located approximately 65 km east inside Corner Inlet (Figure 1). Both gauges are in complex lower-energy environments, where sediment transport, dredging, bathymetry, and other local factors may heavily modify the water levels observed at these tide gauges compared to nearby locations on open coasts (Talke and Jay 2020). Conversely, the Portland gauge is in a well-exposed location on the outer side of the breakwater (Bureau of Meteorology 2020b), unlikely to be subjected to strong riverine or estuarine effects. The effects of local factors on the tidal dynamics of Inverloch are therefore largely unknown. Hence, it is unclear whether it is suitable to use Stony Point or Port Welshpool for the Inverloch analysis, as it unknown how comparable the sites are to Inverloch, despite their relative proximity. Therefore, we have decided to use sea level observations and residual data for Portland for both study locations as it is likely more representative of the broader astronomical forcing and less likely to be heavily influenced by local factors.

The daily maximum residuals (the non-tidal component of the observed sea level) are very highly correlated between Portland, Stony Point and Lorne, the three ABSLMP sites in Victoria. Residuals are commonly-used metrics to identify storm surges, the physical phenomenon typically associated with high still water levels that lead to coastal impacts in Victoria (McInnes et al. 2016; O'Grady et al. 2019a). Pair-wise correlations (using Pearson's R) of 0.86 (Portland-Stony Point), 0.93 (Portland-Lorne) and 0.96 (Lorne-Stony Point) were calculated using data over the 2013-2019 (inclusive) period.

3.3 Coastal Impacts

We consider a broad definition of coastal impacts to reflect the qualitative and sparse nature of the impacts data and considering the diversity of impact definitions used within the literature and perceived by members of the public (Haigh et al. 2017; Hague et al. 2019). Impacts were obtained from social and news media and local interest groups, where photographs demonstrated a loss of beach utility, for example, water reaching the toe of dunes, inundation of beach assets (e.g. steps) and overtopping of sea walls (See Online Resource 1). There is currently no formal reporting system for coastal impacts that enables a comprehensive assessment of when events have and have not occurred.

In each case, photographic or video evidence was used to support claims of coastal impacts occurring (See Online Resource 1). Reports collected only define when a hazardous coastal event has occurred, not the severity of the impacts. To allow for potential uncertainty in the exact time and impact-report was made, we examined a 3-day period centered on the stated reporting date; similar to Hague et al. (2019).

4 Wave Climate Hindcast

Port Fairy has a more energetic wave climate than Inverloch, with an average H_s of 2.45 and 1.74 m and average T_m of 8.43 and 6.73 s respectively. Both sites are dominated by south-westerly waves, but with a more southerly approach in Port Fairy (214^o) and westerly in Inverloch (230^o). Seasonal variability in the wave climate is statistically significant at both sites (Table 2). Average H_s is lowest during Austral summer between November and February (Inverloch: 1.48-1.61 m, Port Fairy: 1.99-2.23 m) and 25% higher during Austral winter from June to August and into September (Inverloch: 1.78-2.03 m, Port Fairy: 2.48-2.86 m) (Figure 3). Wave approach is consistently from a south-westerly direction throughout the year (Inverloch: 222-237^o, Port Fairy: 194-222^o) with only a 5% difference between summer-winter months, that is characterized by more westerly approaches in winter and southerly during summer. T_m increases

from January to April (Inverloch: 9.43-10.14 s, Port Fairy: 9.90-11.53 s) and decreases from September/October back through to January (Inverloch: 10.7-9.42 s, Port Fairy: 11.83-10.65 s); summer-winter conditions differ by ~5% at both sites (Figure 3).

Despite some seasonality, both Port Fairy and Inverloch have an energetic wave climate throughout much of the year (Figure 3). This is consistent with conditions across the Southern Ocean which has a largely spatially homogeneous wave climate and shows minimal seasonal variability compared to similar latitudes in the Northern Hemisphere (Young et al. 2020). As found in Port Fairy and Inverloch, the Southern Ocean experiences only a 25% difference in summer-winter H_s, which is owed to the almost continuous fetch for wind-wave generation in this region (Young et al. 2020).

Table 2: One-way ANOVA analysis results testing for seasonality in H_s, θ_m and $T_{m,}$ in Inverloch and Port Fairy, with each showing $F > F_{crit}$ and $P < 0.05$.

	Port Fairy			Inverloch		
	H_s (m)	θ_m (^{o})	T_m (s)	H_s (m)	θ_m (^{o})	T_m (s)
P	1.45E-34	7.61E-174	3.68E-82	6.94E-42	1.47E-71	1.72E-75
F	63.10	202.71	58.82	25.60	49.13	52.43
F_{crit}	2.62	1.81	1.81	1.80	1.81	1.81

4.1 Sea State

Moderate to high sea states, according to the Douglas Scale (Bureau of Meteorology 2020a),account for 96% of the monthly record in Port Fairy and 70% of the record in Inverloch, with the remainder characterized by calmer conditions. The degree of sea state is negatively correlated with the frequency of occurrence (Port Fairy: r = -0.88, Inverloch: r = -0.84) and positively correlated with the coefficient of variation (Port Fairy: C_v = 0.89, Inverloch: C_v = 0.9),

demonstrating lower frequency but greater variability in rougher conditions (Figure 4). Moderate sea states dominate 54% of the monthly records in Port Fairy and 55% in Inverloch. Rough sea states account for 35% of the record in Port Fairy and 13% in Inverloch. Very rough states account for 6% and 2% and high states 0.3% and 0.07% of the record at Port Fairy and Inverloch respectively. Seasonality is increasingly evident in the record with greater degree of sea state; rough, very rough and high sea states occur more frequently during Austral winter at both sites (Figure 4).

Linear trends in the hourly exceedance of each sea state over the record are negligible (Figure 5), although trends should be treated with caution from the WW3 data due to variations in model versions and input conditions (see Methods and Data). However, Change Point Detection (CPD) analysis shows an increase in the average number of high sea states in June 2008, increasing the average by 62% at both sites (Figure 5). A step change is also identified for very rough sea states in July 2013, increasing by 52% in Inverloch and 66% in Port Fairy (Figure 5). The step change in July 2013 could be a consequence of changes in the model version used in June 2013 (allowing for spin-up), however we also note that there was an increase in reporting of coastal impacts in Inverloch at this time and we are unable to qualify whether the increase in very rough sea states in the record is a model artifact or actual phenomenon.

5 Comparing Typical And Impact-producing Oceanic Conditions

A total of 10 coastal impact events have been identified in Port Fairy between January 2009 and June 2020 and a total of 20 events have been identified in Inverloch between January 2012 and June 2020; the analysis herein for each site has therefore been restricted to these periods. Impacts were identified using the methods outlined in Section 3.3 and pertain to loss of beach utility at each site. See Online Resource 1 and 2 for details related to each event.

Here we compare the distributions of key oceanographic parameters during these periods of impacts to the distribution across all hourly WW3 outputs. So that the two distributions are comparable at each site, we use a period of 2009-2020 for Port Fairy analysis and 2012-2020 for Inverloch.

Table 3: Statistics for wave, sea level and residual conditions in Port Fairy from the WW3 outputs for the period 2009-2020 (Port Fairy), 2012-2020 (Inverloch) and for event data at both sites.

Site	Wave, Sea Level and Residual Conditions		Mean	Median	Mode1	Mode2	Standard Deviation	Variance	Skew	Kurtosis
Port Fairy	Hs (m)	*2009-2020*	2.56	2.37	1.99	-	0.96	0.92	1.03	4.20
		events	2.89	2.82	1.85	2.95	1.11	1.24	0.50	3.79
	θ_m (º)	*2009-2020*	218	218	220	-	10.81	116.91	-0.71	5.11
		events	221	222	225	-	11.84	140.2	-0.20	2.38
	Tm (s)	*2009-2020*	8.84	8.76	8.62	-	1.63	2.66	0.34	3.05
		events	8.95	8.94	7.69	9.30	1.51	2.28	0.26	2.34
	HT (m)	*2009-2020*	0.82	0.80	0.74	-	0.17	0.03	0.10	2.57
		events	0.86	0.80	0.76	-	0.16	0.03	0.50	2.14
	RES (m)	*2009-2020*	0.00	-0.01	-0.01	-	0.12	0.01	0.36	3.33
		events	0.07	0.08	0.12	-	0.17	0.03	-0.1	2.08
Inverloch	Hs (m)	*2012-2020*	1.84	1.63	1.35	-	0.86	0.73	1.49	5.82
		events	2.80	2.57	2.06	-	1.29	1.65	0.50	2.33
	θ_m (º)	*2012-2020*	231	232	231	-	14.74	217.39	-1.38	8.55
		events	238	239	229	241	10.08	101.67	0.08	2.73
	Tm (s)	*2012-2020*	6.94	6.66	6.47	-	1.66	2.75	0.84	3.64
		events	6.81	6.74	6.61	-	0.99	0.97	0.55	4.72
	HT (m)	*2012-2020*	0.82	0.80	0.75	-	0.17	0.03	0.14	2.55
		events	0.86	0.83	0.76	-	0.16	0.03	0.41	2.83
	RES (m)	*2012-2020*	0.00	-0.01	-0.01	-	0.12	0.01	0.35	3.27
		events	0.05	0.04	0.02	-	0.14	0.02	0.13	2.23

5.1 Port Fairy

H_s between 2009-2020 has a negative unimodal distribution with a modal value of 1.99 m and higher mean and median values of 2.56 and 2.37 m respectively (Table 3, Figure 6a). The mean value is higher than observed between 1979-2020 (2.45 m), although these differences should be taken with caution given that trends in the WW3 hindcast

could be influenced by changes in model version and input conditions. H_s recorded during known events have a higher central tendency compared to the 2009-2020 period, with a mean of 2.89 m (Table 3). The distribution is bimodal however and shows peaks at 1.85 m and 2.95 m, with the former below the mode of the 2009-2012 dataset. On average, H_s during events falls within the 63rd percentile (2.71 m) of the 2009-2012 dataset, demonstrating that H_s is consistently higher during events compared to the mean conditions in Port Fairy and falls within the 'Rough' sea state category according to the Douglas Scale (Bureau of Meteorology 2020a).

θ_m has a unimodal distribution and analogous measures of central tendency with a mean of 217^o, denoting a dominant southwesterly wave approach (Table 3, Figure 6b). θ_m is therefore shown to be marginally more westerly during 2009-2020 than calculated over the 1979-2020 period (214^o). θ_m recorded during known events has a mean of 221^o, demonstrating that events tend to occur when waves approach from a more westerly direction. The wave direction has an average percentile ranking of 60% (221^o), influenced by a plateau at 209^o, but the percentile ranking of the primary peak is 77% (225^o). Approximately 43% of events occur under a more southerly wave approach and 57% under a more westerly approach compared to the 2009-2020 modal conditions.

T_m between 2009-2020 is unimodal with a mean of 8.84 s (Table 3, Figure 6c), longer than observed between 1979-2020. T_m recorded during known events is comparable to the 2009-2020 conditions, but with a marginally higher mean at 8.95 s. The distribution of event data is bimodal, with peaks below the 2009-2020 mean at 7.69 s and above, at 9.30 s. This bimodality influences the average percentile ranking, calculated at 54% (8.93 s).

Mean high tide (HT) between 2009-2020 is 0.82 m and during recorded events is higher at 0.86 m (Table 3, Figure 6d). Event data also has a higher positive skew due to the clustering of conditions around 0.95-1.05 m. On average, high tides recorded during events are ranked in the 59th percentile (0.85 m) of the entire dataset.

The distribution of tidal residuals (RES) is relatively symmetrical, with central tendencies ranging between 0.00 and -0.01 m (Table 3, Figure 6e). There is some skew in the dataset due to the occurrence of higher-residual conditions at +0.40 m. Residual levels during events tend to be higher and have a mean value of 0.07 m. On average, residuals during events rank in the 65th percentile (0.04 m) within the 2009-2020 dataset. Residual elevations and wave directions recorded during events are positively correlated with a Pearson's R value of 0.74. Higher residuals are therefore associated with more westerly wave approaches.

5.2 Inverloch

H_s has a positively skewed unimodal distribution with a mean of 1.84 m; mean H_s for the period 2012-2020 (Table 3, Figure 6f) is higher than observed between 1979-2020 (1.74 m), although trends in the dataset should be taken with caution as noted previously. H_s during events have higher central tendencies compared to the period 2012-2020, with a mean of 2.80 m and an average percentile ranking of 82% (2.47 m) within the 2012-2020 dataset. This demonstrates that H_s is consistently higher during events compared to the mean conditions in Inverloch and falls within the 'Rough' sea state category according to the Douglas Scale (Bureau of Meteorology 2020a)..

The distribution of wave directions between 2012-2020 is negatively skewed and has analogous central tendency values between 231-232^o (Table 3, Figure 6g). This denotes a dominant and relatively consistent southwesterly wave direction, but with few occurrences from a more southerly approach. The average direction recorded between 2012-2020 is comparable to the mean conditions for 1979-2020 (230^o) (Table 2). The mean and median wave directions

during known events are near-equivalent at 238-239°. The wave direction has an average percentile ranking of 69% (237°), influenced by the first (36th) and second (80th) modal peaks. The average percentile ranking for events is more westerly than the modal value for the 2012-2020 period (231°, 44th), with only 20% of event cases occurring with a more southerly approach than the modal conditions and the remainder approaching from a more westerly direction (Figure 6g).

T_m between 2012-2020 is positively skewed, with a mean value of 6.94 s (Table 3, Figure 6h); marginally longer than T_m for 1979-2020 calculated at 6.73 s (Table 2). The range of wave periods recorded during events is narrower than over the 2012-2020 period and has a marginally shorter mean value of 6.81 s. T_m during events has an average percentile ranking of 53% (6.78 s) within the 2012-2020 dataset (Figure 6h).

Mean HT between 2012-2020 is 0.82 m and during recorded events is marginally higher at 0.86 m (Table 3, Figure 6i). The distribution of data for the 2012-2020 period and for events is comparable, but event data has a greater positive skew with more instances at higher HT levels. On average, HT levels recorded during events are ranked in the 68th percentile within the 2012-2020 dataset (0.85 m).

Mean tidal residual elevations (RES) during HT between 2012-2020 is 0.00 m and for recorded events, is 0.05 m (Table 3, Figure 6j). The distribution is leptokurtic for the 2012-2020 period, but more platykurtic for events, plateauing between 0.03-0.2 m. On average, residuals during events rank in the 62nd percentile (0.04 m) of the 2012-2020 dataset. Residual elevations and wave directions recorded during events are positively correlated with a Pearson's R value of 0.76. Higher residuals are therefore associated with more westerly wave approaches and as shown previously, the majority of events occur where there is a more westerly wave direction.

6 Discussion: Can Ocean Conditions Be Used As A Proxy For Coastal Impacts?

We can identify similarities and differences in the drivers of impact-producing extreme total water levels and oceanic conditions in Port Fairy and Inverloch. Impact-producing events are associated with higher-than-average wave heights at both sites, which are 15% above average in Port Fairy and 52% in Inverloch. Whilst events in Inverloch have a greater above-average H_s, the values are similar at 2.89 m and 2.80 m for Port Fairy and Inverloch respectively, demonstrating that similar H_s are conducive to coastal impacts at both sites. According to the Douglas Scale, these H_s values fall within the 'Rough' sea state category (Bureau of Meteorology 2020a). These conditions appear more extreme in Inverloch due to the, generally, calmer wave conditions within Bass Strait owing to wave blocking, shorter fetch and the wide, shallow continental shelf (McSweeney 2020).

The mean direction of wave approach at both sites is southwesterly, with events occurring under a more westerly wave direction than the mean. The influence of wave direction on impact-occurrence has been well documented along the east coast of Australia, following the 2016 East Coast Low storm. Harley et al., (2017) demonstrated that storm wave direction and the local shoreline orientation significantly influenced the degree of impacts along the east coast due to the modulation of wave exposure. In fact, wave direction was considered a more significant factor in generating coastal impacts along Australian's east coast during the 2016 East Coast Low compared to the wave height, which was not considered to be exceptionally high for this region (Mortlock et al. 2017). Although a more westerly wave approach in Port Fairy and Inverloch would seemingly reduce exposure due to the local shoreline orientation, waves tracking from this direction are likely to have more energy due to the unique wind-wave climate that traverses the Southern Ocean (Young et al. 2020). Degree of exposure is also influenced by blocking (Young et al.

2020) within Bass Strait, where Tasmania and other offshore Islands have been shown to reduce wave propagation from the South (McSweeney 2020). These effects are evident in the results, owing to the fact that directionality has a lesser influence on event occurrence in Port Fairy with only 57% of events occurring under a more westerly wave climate, compared to 80% in Inverloch. Inverloch experiences these blocking effects within Bass Strait and is therefore more sensitive to the wave direction, with westerly waves being less inhibited than southerly waves.

Coastal impact events in Port Fairy were typically associated with higher-than-average wave periods (1% higher), but in Inverloch, were lower than average (-2%). Marginal difference from the mean conditions suggests that the wave period is not the most pivotal factor in inducing impacts at either site. This could be due to other factors being more dominant, a lack of observations or due to use of the mean rather than the peak period. This is particularly relevant in Port Fairy which shows bimodality in the wave period, therefore showing the average of two wave trains as opposed to the most energetic conditions per se.

Both locations saw impacts coincide with periods of above-average still water levels, particularly associated with residual elevations (tides: 5% higher, residuals: -3357-8258% higher). Coastal impacts have shown to be amplified when storm occurrence coincides with anomalously high sea levels (Hoeke et al. 2013). However, this is not something that is ostensibly true for all coastal locations where other factors, such as wave exposure (Harley et al. 2017), local bathymetry (Kennedy et al. 2012; Kennedy 2016), swell-wave propagation (Hoeke et al. 2013), sediment composition (Wright and Short 1984), coastal orientation (Masselink et al. 2016) and geological controls (Jackson et al. 2005; Gallop et al. 2020) can play a more pivotal role in impact occurrence or severity at specific sites.

The wave conditions identified herein as conducive to causing an impact on the coast at Inverloch and Port Fairy are predicted to occur more frequently in the future, in particular, higher significant wave heights (Morim et al. 2019) and still water levels (Wong et al. 2015). Along the coast of Victoria, future increases in storm frequency and magnitude are likely to induce greater coastal impacts on sandy landforms. Predictions of a southerly rotation in the wave climate (Morim et al. 2019) could lead to different responses of these two sites as well as other beaches and dunes along this stretch of coastline. The majority of events in Inverloch occur under a more westerly wave approach, but more westerly-driven events only have a 7% dominance over more southerly events in Port Fairy, compared with the mean southwesterly conditions. Port Fairy is therefore more likely to be sensitive to future southerly shifts in the wave climate (Leach et al. 2020) compared to Inverloch, which experiences a more complex wave environment within Bass Strait with offshore islands affording some southerly protection (McSweeney, 2020).

The conditions identified as being conducive to impacts in Port Fairy and Inverloch differ and will likely vary from impact-inducing conditions in other parts of the world. Therefore, not only is identifying spatial variations in oceanic conditions important to quantify coastal risk but identifying how day-to-day variations away from these longer-term climatological conditions affect coastal impacts is also necessary. They key is identifying the unique set of conditions that lead to impacts at the regional or site-specific level. These goals would be unobtainable without impact data and whilst this study has been limited by the sparsity and informality of evidence, we have nevertheless been able to isolate patterns and consistencies in conditions that occur during known events in Port Fairy and Inverloch that could be used to inform impacts in future scenarios and forecasts. We demonstrate the benefits in incorporating impact data into coastal risk assessments and highlight the need to develop comprehensive databases and methods for reporting impacts in coastal areas. This would include when events do and do not occur as well as quantitative measures of the nature and severity of impacts observed.

7 Future Directions: The Need For Impact-based Insights Into Coastal Hazards

Using a correlative approach that does not consider the specifics of local conditions, we have shown herein that the oceanic conditions that lead to coastal impacts vary in two case study sites along the Victorian coastline. We have achieved this, even with the relatively limited amount of impact-based data available. In order for the assumption of spatial coherency in coastal impacts to be examined more closely, more impact information needs to be made available, or generated. Ultimately, this means a more comprehensive list of events is required to develop impact-based insights. Social media data has been increasingly used as a source of information on the impacts of climatic, meteorological and oceanographic phenomena, primarily flooding, for early warning and event monitoring systems, and for future preparedness (Middleton et al. 2014; Haigh et al. 2017; Smith et al. 2017; Rossi et al. 2018; de Bruijn et al. 2019; Moore et al. 2019; Moore and Obradovich 2020). Prior to the advent of social media, impacts have been similarly documented using news media archives (Callaghan and Power 2014; Haigh et al. 2017).

Like other observational and model datasets alike, social media datasets can suffer from biases. One such bias is that the remarkability, and hence one's likelihood to post about the impacts of an event, can decline if the event becomes commonplace. For example, Moore et al. (2019) found that the remarkability of an event was typically judged against the previous decade. Hence, the public perception of increasingly frequent and severe impacts could be skewed by the shifting baselines of normalcy, against which the extremeness and remarkability of a particular event are assessed. However, such news and social media-based assessments of impacts have been shown to deliver comparable results to those using conventional threshold-based (Moore and Obradovich 2020) or modelling (Habel et al. 2020; Yagoub et al. 2020) approaches. Moore and Obradovich (2020) identified some circumstances where flood thresholds derived using social media observations were more representative of the vertical height at which impacts typically associated with minor flood occur, than the actual defined minor thresholds. This indicates that when viewed from an impact-based perspective, metrics that have less of a reliance of impact information may be overall more biased than those obtained using social and news media reports.

Citizen science programs such as the VCMP (DELWP 2019) and CoastSnap (Harley et al. 2019) as well as new techniques for utilizing existing coastal cameras to produce qualitative estimates of coastal change (Dusek et al. 2019; Conlin et al. 2020), means that this impact data will become more readily available as impact-producing ESLs occur in the future. Such an impact-based approach may be desirable for several reasons. Firstly, it may be less computationally and financially expensive than detailed, high-resolution modelling and be simpler to apply in real-time by local coastal managers. This would also enable it to be implemented on a more global-scale. Secondly, it has been shown that incorporating impacts data can lead to insights into to coastal risk that would be otherwise not available through conventional risk assessment and modelling activities (Moore and Obradovich 2020). Thirdly, it can engage local citizen science groups to take an interest in the natural hazards affecting their local area which can lead to auxiliary benefits to the local residents, the coordinating scientists and local managers and policy makers (Guerrini et al. 2018; Sagy et al. 2019).

Beyond just impact-based data, there is a demand for increased coastal observations more generally. Priority areas identified across Australia have included improved wave and sea state observations facilitated through the maintenance and enhancement of the wave buoy network, long-term beach and coastline monitoring, mapping nearshore and coastal bathymetry, conducting geomorphological assessments, mapping coastal ecosystems and identifying thresholds for impacts in the coastal zone (COAG 2006; IMOS 2016; Greenslade et al. 2020). There is also a need for a more coordinated approach to data collection, storage and sharing. Acquiring information, research outputs and datasets from different agencies can be challenging and often, research or data collection is duplicated. A core goal of Australia's Integrated Marine Observing System (IMOS) is to address this issue by providing a central location where data are collated for ease of discovery, accessibility and use (IMOS 2016). Access to these resources

across Australia, and globally, will lead to improved knowledge of coastal systems and associated impacts, as well as more effective decision-making about suitable and sustainable management practices (COAG 2006).

8 Conclusion

Whilst many studies have investigated future extreme sea levels on Australian and global coastlines, few have considered empirical impact data in their methodology, despite these impacts being the motivating factor for such research. Here, we have isolated the conditions that have occurred during known events at two temperate, high energy sandy beach backed by foredunes in southeast Australia: Port Fairy and Inverloch. We have identified differences in the energetics of the wave climate and effects of blocking between both locations and that different variations on daily scales, away from the mean climate, have different effects within and between both locations. However, the data also shows that at both sites, impacts occur namely when there is higher-than-average still water levels and higher waves. This suggests that impactful events might be very sensitive to continued sea-level rise into the future. Such insights are predicated on identifying past coastal impact events, primarily from social media, and assessing the oceanographic conditions that coincided with these impact events.

This study demonstrates that impact data is required for studies into impact-inducing oceanic conditions. It also shows that there is potential for erosion risk matrices or other impact-relevant early warning systems to be used in the Australian context. This however will require large-scale efforts to collate and analyse impact data from coastal impact hotspots from around Australia. Such infrastructure and technology have emerged in recent years, meaning this may become viable as the volume of impact data reaches a critical level. By identifying the oceanic conditions that are conducive to impacts on the open coast we have shown the potential for the future development of operational warning systems to be established for the hazards associated with extreme total water levels along the open coasts of Victoria, Australia, and potentially, further afield.

9 Declarations

Funding

Research funds for this project were provided by the Victorian Department of Environment, Land, Water and Planning as part of the Victorian Coastal Monitoring Program (VCMP) supported by the Sustainability Fund, Deakin University and the University of Melbourne.

Conflicts of interest/Competing interests

The authors declare that there is no conflict of interest.

Availability of data and material

The datasets used and/or analysed during the current study are available from the corresponding author on request.

Code availability

Not applicable.

Authors' contributions

Material preparation, data collection and analysis were performed by Chloe Leach and Ben Hague. The first draft of the manuscript was written by Chloe Leach and Ben Hague and all authors commented and provided contributions to all versions of the manuscript. All authors read and approved the final manuscript.

Ethics Approval

Not Applicable.

Consent to participate

Not Applicable.

Consent for publication

Not Applicable.

Acknowledgements

This project was funded by the Victorian Department of Environment, Land, Water and Planning as part of the Victorian Coastal Monitoring Program (VCMP) supported by the Sustainability Fund, Deakin University and the University of Melbourne. The authors would like to thank Diana Greenslade and Grant Smith whose reviews contributed to improvements in the manuscript.

10 References

Allen SCR, Greenslade DJM (2016) A Pilot Tsunami Inundation Forecast System for Australia. In: Global Tsunami Science: Past and Future. Birkhäuser, Cham, pp 3955–3971

Australian Hydrographic Service (2012) Australian National Tide Tables 2013. Department of Defence, Commonwealth of Australia

Bureau of Meteorology (2020a) Waves. http://www.bom.gov.au/marine/knowledge-centre/reference/waves.shtml. Accessed 26 Oct 2020

Bureau of Meteorology (2021) Australian Baseline Sea Level Monitoring Project Hourly Sea Level and Meteorological Data. http://www.bom.gov.au/oceanography/projects/abslmp/data/index.shtml. Accessed 5 Jan 2021

Bureau of Meteorology (2020b) Monthly Data Report – August 2020. http://www.bom.gov.au/ntc/IDO60201/IDO60201.202008.pdf. Accessed 26 Oct 2020

Callaghan J, Power SB (2014) Major coastal flooding in southeastern Australia 1860–2012, associated deaths and weather systems. Aust Meteorol Oceanogr J 64:183–213

Carvalho RC, Kennedy DM, Niyazi Y, et al (2020) Structure-from-motion photogrammetry analysis of historical aerial photography: Determining beach volumetric change over decadal scales. Earth Surf Process Landforms. https://doi.org/10.1002/esp.4911

Church JA, Hunter JR, McInnes KL, White NJ (2006) Sea-level rise around the Australian coastline and the changing frequency of extreme sea-level events. Aust Meteorol Mag

COAG (2006) National Climate Change Adaptation Framework. Canberra, Australia

Conlin MP, Adams PN, Wilkinson B, et al (2020) SurfRCaT: A tool for remote calibration of pre-existing coastal cameras to enable their use as quantitative coastal monitoring tools. SoftwareX 12:100584. https://doi.org/10.1016/j.softx.2020.100584

de Bruijn JA, de Moel H, Jongman B, et al (2019) A global database of historic and real-time flood events based on social media. Sci data 6:. https://doi.org/10.1038/s41597-019-0326-9

DELWP (2019) Victorian Coastal Monitoring Program. https://www.marineandcoasts.vic.gov.au/coastal-programs/victorian-coastal-monitoring-program. Accessed 23 Dec 2020

Devlin AT, Jay DA, Talke SA, et al (2017) Coupling of sea level and tidal range changes, with implications for future water levels. Sci Rep 7:. https://doi.org/10.1038/s41598-017-17056-z

Doumtsis S (2020) Beach dynamics in response to varying boundary conditions: the role of rocks and tidal deltas. Masters Thesis, University of Melbourne

Durrant T, Hemer M, Trenham C, Greenslade D (2013) CAWCR Wave Hindcast 1979–2010. CSIRO. Service Collection. https://doi.org/102.100.100/13165

Dusek G, Hernandez D, Willis M, et al (2019) WebCAT: Piloting the development of a web camera coastal observing network for diverse applications. Front Mar Sci 6:353. https://doi.org/10.3389/fmars.2019.00353

Flocard F, Carley J., Rayner D., et al (2013) Future Coasts: Port Fairy Coastal Hazard Assessment. Water Res Lab Sch Civ Environ Eng

Gallop SL, Kennedy DM, Loureiro C, et al (2020) Geologically controlled sandy beaches: Their geomorphology, morphodynamics and classification. Sci Total Environ 731:139123. https://doi.org/10.1016/j.scitotenv.2020.139123

Greenslade D, Hemer M, Babanin A, et al (2020) 15 priorities for wind-waves research: An Australian perspective. Bull Am Meteorol Soc 101:E446–E461. https://doi.org/10.1175/BAMS-D-18-0262.1

Guerrini CJ, Majumder MA, Lewellyn MJ, McGuire AL (2018) Citizen science, public policy. Science (80-) 361:134–136

Habel S, Fletcher CH, Anderson TR, Thompson PR (2020) Sea-Level Rise Induced Multi-Mechanism Flooding and Contribution to Urban Infrastructure Failure. Sci Rep 10:. https://doi.org/10.1038/s41598-020-60762-4

Hague B, McGregor S, Murphy BF, et al (2020) Sea-Level Rise Driving Increasingly Predictable Coastal Inundation in Sydney, Australia. Earth's Futur 8:. https://doi.org/10.1029/2020EF001607

Hague BS, Murphy BF, Jones DA, Taylor AJ (2019) Developing impact-based thresholds for coastal inundation from tide gauge observations. J South Hemisph Earth Syst Sci 69:252–72. https://doi.org/10.1071/es19024

Haigh ID, Ozsoy O, Wadey MP, et al (2017) An improved database of coastal flooding in the United Kingdom from 1915 to 2016. Sci Data 4:. https://doi.org/10.1038/sdata.2017.100

Harker A, Green JAM, Schindelegger M, Wilmes S-B (2019) The impact of sea-level rise on tidal characteristics around Australia. Ocean Sci 15:147–159. https://doi.org/10.5194/os-15-147-2019

Harley MD, Kinsela MA, Sánchez-García E, Vos K (2019) Shoreline change mapping using crowd-sourced smartphone images. Coast Eng 150:175–189. https://doi.org/10.1016/j.coastaleng.2019.04.003

Harley MD, Turner IL, Kinsela MA, et al (2017) Extreme coastal erosion enhanced by anomalous extratropical storm wave direction. Sci Rep 7:1–9. https://doi.org/10.1038/s41598-017-05792-1

Hemer MA, Church JA, Hunter JR (2010) Variability and trends in the directional wave climate of the Southern Hemisphere. Int J Climatol 30:475–91. https://doi.org/10.1002/joc.1900

Hemer MA, Griffin DA (2010) The wave energy resource along Australia's Southern margin. J Renew Sustain Energy 2:043108. https://doi.org/10.1063/1.3464753

Hoeke RK, McInnes KL, Kruger JC, et al (2013) Widespread inundation of Pacific islands triggered by distant-source wind-waves. Glob Planet Change 108:128–138. https://doi.org/10.1016/j.gloplacha.2013.06.006

Hughes MG, Heap AD (2010) National-scale wave energy resource assessment for Australia. Renew Energy 35:1783–1791. https://doi.org/10.1016/j.renene.2009.11.001

IMOS (2016) IMOS Five Year Plan (2017-22). https://imos.org.au/about/plans-and-reports/imos-five-year-plan-2017-22. Accessed 23 Feb 2021

Jackson DWT, Cooper JAG, Del Rio L (2005) Geological control of beach morphodynamic state. Mar Geol 216:297–314. https://doi.org/10.1016/j.margeo.2005.02.021

Kennedy AB, Westerink JJ, Smith JM, et al (2012) Tropical cyclone inundation potential on the Hawaiian Islands of Oahu and Kauai. Ocean Model 52:. https://doi.org/10.1016/j.ocemod.2012.04.009

Kennedy DM (2016) The subtidal morphology of microtidal shore platforms and its implication for wave dynamics on rocky coasts. Geomorphology 268:146–158. https://doi.org/10.1016/j.geomorph.2016.06.003

Kirezci E, Young IR, Ranasinghe R, et al (2020) Projections of global-scale extreme sea levels and resulting episodic coastal flooding over the 21st Century. Sci Rep 10:1–12. https://doi.org/10.1038/s41598-020-67736-6

Konlechner TM, Kennedy DM, O'Grady JJ, et al (2020) Mapping spatial variability in shoreline change hotspots from satellite data; a case study in southeast Australia. Estuar Coast Shelf Sci 246:107018. https://doi.org/10.1016/j.ecss.2020.107018

Leach C, Kennedy DM, Carvalho RC, Ierodiaconou D (2020) Predicting Compartment-scale Climate Change Impacts Related to Southern Ocean Wave Forcing: Port Fairy, Victoria, Australia. J Coast Res 95:1157–1161. https://doi.org/10.2112/SI95-224.1

Marshall AG, Hemer MA, Hendon HH, McInnes KL (2018) Southern annular mode impacts on global ocean surface waves. Ocean Model 129:. https://doi.org/10.1016/j.ocemod.2018.07.007

Marshall AG, Hemer MA, McInnes KL (2020) Australian blocking impacts on ocean surface waves. Clim Dyn 54:. https://doi.org/10.1007/s00382-019-05058-8

Marshall AG, Hendon HH, Durrant TH, Hemer MA (2015) Madden Julian Oscillation impacts on global ocean surface waves. Ocean Model 96:. https://doi.org/10.1016/j.ocemod.2015.06.002

Masselink G, Scott T, Poate T, et al (2016) The extreme 2013/2014 winter storms: Hydrodynamic forcing and coastal response along the southwest coast of England. Earth Surf Process Landforms 41:378–391. https://doi.org/10.1002/esp.3836

McInnes KL, Church J, Monselesan D, et al (2015) Information for Australian Impact and Adaptation Planning in response to Sea-level Rise. Aust Meteorol Oceanogr J 65:127–149. https://doi.org/10.22499/2.6501.009

McInnes KL, White CJ, Haigh ID, et al (2016) Natural hazards in Australia: sea level and coastal extremes. Clim Change 139:69–83. https://doi.org/10.1007/s10584-016-1647-8

McSweeney SL (2020) Temporal and spatial variability of the open coast wave climate of Victoria, Australia. Mar Freshw Res 71:394–413. https://doi.org/10.1071/MF18489

Meucci A, Young IR, Hemer M, et al (2020) Projected 21st century changes in extreme wind-wave events. Sci Adv 6:7295–7305. https://doi.org/10.1126/sciadv.aaz7295

Middleton SE, Middleton L, Modafferi S (2014) Real-time crisis mapping of natural disasters using social media. IEEE Intell Syst 29:. https://doi.org/10.1109/MIS.2013.126

Moore FC, Obradovich N (2020) Using remarkability to define coastal flooding thresholds. Nat Commun 11:1–8. https://doi.org/10.1038/s41467-019-13935-3

Moore FC, Obradovich N, Lehner F, Baylis P (2019) Rapidly declining remarkability of temperature anomalies may obscure public perception of climate change. Proc Natl Acad Sci U S A 116:. https://doi.org/10.1073/pnas.1816541116

Morim J, Hemer M, Wang XL, et al (2019) Robustness and uncertainties in global multivariate wind-wave climate projections. Nat Clim Chang 9:711–718. https://doi.org/10.1038/s41558-019-0542-5

Mortlock T, Goodwin I, McAneney J, Roche K (2017) The June 2016 Australian East Coast Low: Importance of Wave Direction for Coastal Erosion Assessment. Water 9:121. https://doi.org/10.3390/w9020121

Muis S, Apecechea MI, Dullaart J, et al (2020) A High-Resolution Global Dataset of Extreme Sea Levels, Tides, and Storm Surges, Including Future Projections. Front Mar Sci 7:263. https://doi.org/10.3389/fmars.2020.00263

O'Grady JG, McInnes KL, Hemer MA, et al (2019a) Extreme Water Levels for Australian Beaches Using Empirical Equations for Shoreline Wave Setup. J Geophys Res Ocean 124:5468–5484. https://doi.org/10.1029/2018JC014871

O'Grady JG, McInnes KL, Hemer MA, et al (2019b) Extreme Water Levels for Australian Beaches Using Empirical Equations for Shoreline Wave Setup. J Geophys Res Ocean 124:5468–5484. https://doi.org/10.1029/2018JC014871

Pickering MD, Horsburgh KJ, Blundell JR, et al (2017) The impact of future sea-level rise on the global tides. Cont Shelf Res 142:50–68. https://doi.org/10.1016/j.csr.2017.02.004

Pörtner H-O, Roberts, Debra C, Masson-Delmotte V, et al (2019) IPCC Special Report on the Ocean and Cryosphere in a Changing Climate. eds

Ranasinghe R (2016) Assessing climate change impacts on open sandy coasts: A review. Earth-Science Rev 160:320–332. https://doi.org/10.1016/J.EARSCIREV.2016.07.011

Rossi C, Acerbo FS, Ylinen K, et al (2018) Early detection and information extraction for weather-induced floods using social media streams. Int J Disaster Risk Reduct 30:. https://doi.org/10.1016/j.ijdrr.2018.03.002

Sagy O, Golumbic YN, Ben-Horin Abramsky H, et al (2019) Citizen Science: An Opportunity for Learning in the Networked Society. In: Kali Y, Baram-Tsabari A, Schejter A (eds) Learning In a Networked Society. Springer, Cham, pp 97–115

Short AD (2020) Australian Coastal Systems. Springer International Publishing, Cham

Smith L, Liang Q, James P, Lin W (2017) Assessing the utility of social media as a data source for flood risk management using a real-time modelling framework. J Flood Risk Manag 10:. https://doi.org/10.1111/jfr3.12154

South Gippsland Conservation Society Inc. (2020) Inverloch Beach Monitoring Report Inverloch Coastal Resilience Project. www.sgcs.org.au. Accessed 9 Oct 2020

Stephens SA, Bell RG, Haigh ID (2020) Spatial and temporal analysis of extreme storm-tide and skew-surge events around the coastline of New Zealand. Nat Hazards Earth Syst Sci 20:783–796. https://doi.org/10.5194/nhess-20-783-2020

Talke SA, Jay DA (2020) Changing Tides: The Role of Natural and Anthropogenic Factors. Ann Rev Mar Sci 12:121–151. https://doi.org/10.1146/annurev-marine-010419-010727

VCMP (2020) Vicwaves. https://vicwaves.com.au/. Accessed 26 Oct 2020

Wong PP, Losada IJ, Gattuso JP, et al (2015) Coastal systems and low-lying areas. In: Climate Change 2014 Impacts, Adaptation and Vulnerability: Part A: Global and Sectoral Aspects. pp 361–410

Wright LD, Short AD (1984) Morphodynamic variability of surf zones and beaches: A synthesis. Mar Geol 56:93–118. https://doi.org/10.1016/0025-3227(84)90008-2

Yagoub MM, Alsereidi AA, Mohamed EA, et al (2020) Newspapers as a validation proxy for GIS modeling in Fujairah, United Arab Emirates: identifying flood-prone areas. Nat Hazards 104:. https://doi.org/10.1007/s11069-020-04161-y

Young IR, Fontaine E, Liu Q, Babanin AV (2020) The Wave Climate of the Southern Ocean. J Phys Oceanogr 50:1417–1433

Supplementary Material

Online Resource 2: List of known coastal impact events based on demonstrated loss of beach utility and associated oceanic conditions in Port Fairy (2009-2020) and Inverloch (2012-2020).

	Date	Hs (m)	θ_m (°)	Tm (s)	HT (m)	RES (m)
Port Fairy	27/05/2009	3.93	216.10	8.86	0.95	-0.09
	01/06/2009	3.08	233.71	8.44	0.74	-0.16
	21/06/2014	2.27	233.40	9.18	0.84	0.21
	22/07/2016	2.61	223.90	9.49	0.92	0.21
	04/08/2017	3.46	208.26	9.82	0.85	0.24
	01/09/2018	3.63	227.99	10.36	0.81	-0.12
	29/03/2020	3.76	220.72	8.53	0.85	0.03
	06/05/2020	2.63	231.68	8.93	0.86	0.11
	07/05/2020	1.31	215.55	8.59	0.91	0.21
	01/06/2020	2.17	203.10	7.35	0.77	0.07
Inverloch	29/08/2012	2.80	239.16	6.66	0.76	0.05
	15/07/2014	2.80	245.11	6.95	0.91	0.11
	26/07/2016	3.19	240.44	6.84	0.83	0.08
	05/07/2018	3.65	247.76	6.85	0.84	0.26
	06/07/2018	4.40	239.42	7.29	0.82	0.25
	23/03/2019	2.65	243.36	6.68	0.86	0.15
	24/04/2019	3.21	235.84	7.66	0.88	0.04
	25/05/2019	3.48	244.83	6.66	0.86	0.19
	17/06/2019	2.06	233.91	7.01	0.95	-0.05
	09/07/2019	2.92	253.52	6.09	0.82	0.16
	23/07/2019	2.95	242.61	7.33	0.87	0.09
	20/08/2019	4.15	235.60	7.48	0.88	-0.05
	07/09/2019	3.17	234.57	6.42	0.80	0.04
	09/09/2019	2.28	230.65	7.31	0.79	-0.14
	05/04/2020	2.18	229.85	6.30	0.75	0.03
	09/04/2020	2.25	229.47	6.59	0.88	-0.05
	10/04/2020	2.64	233.56	6.21	0.91	-0.03
	05/05/2020	1.23	244.88	6.49	0.82	-0.01
	08/05/2020	2.58	244.77	6.65	0.94	0.19
	23/05/2020	1.50	223.93	6.74	0.96	-0.12

Figures

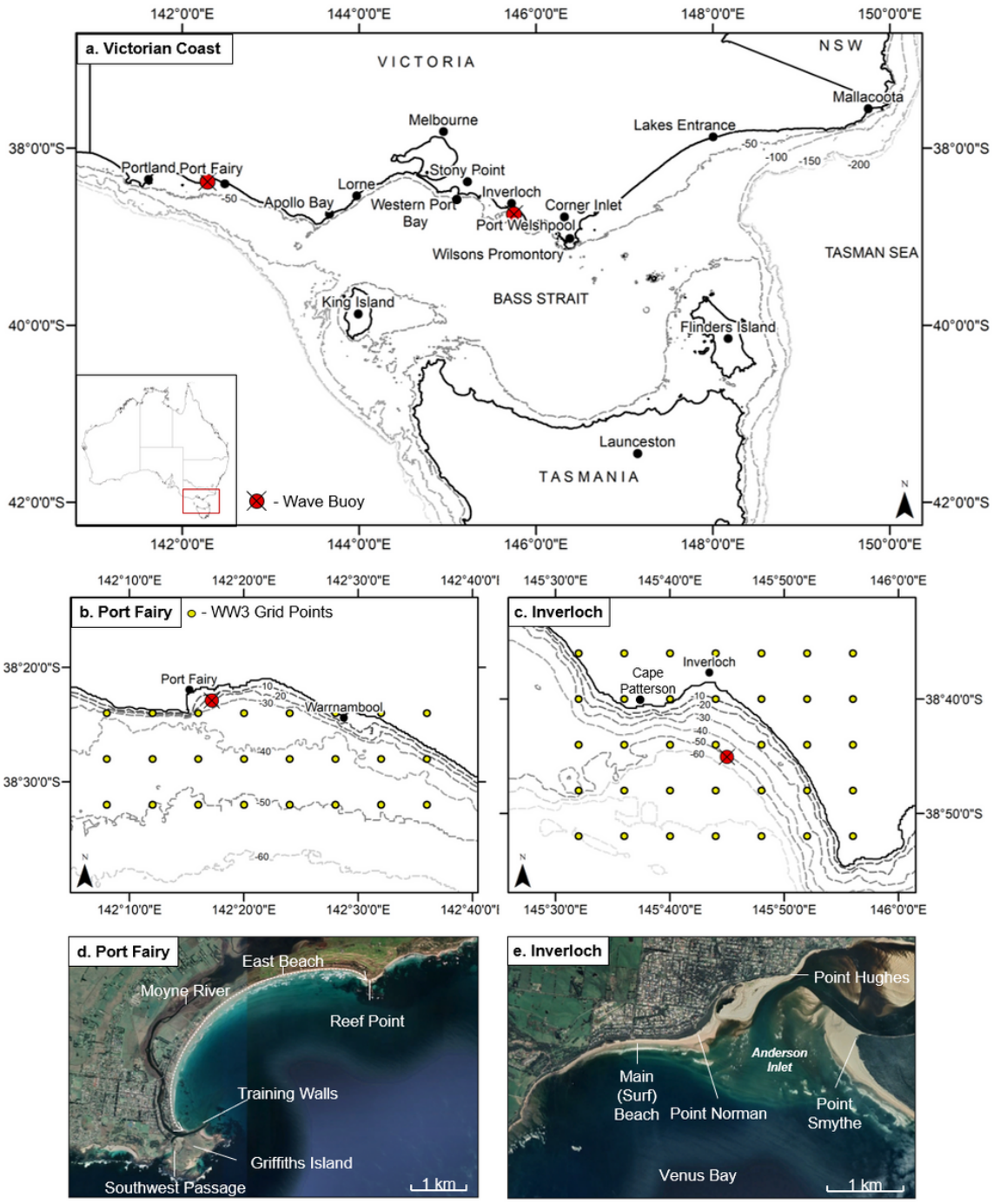

Figure 1

Map of the Victorian Coast, Australia (a), showing the location of the wave buoys and WW3 grid points in Port Fairy (b) and Inverloch (c) and features of interest at both sites (d,e).

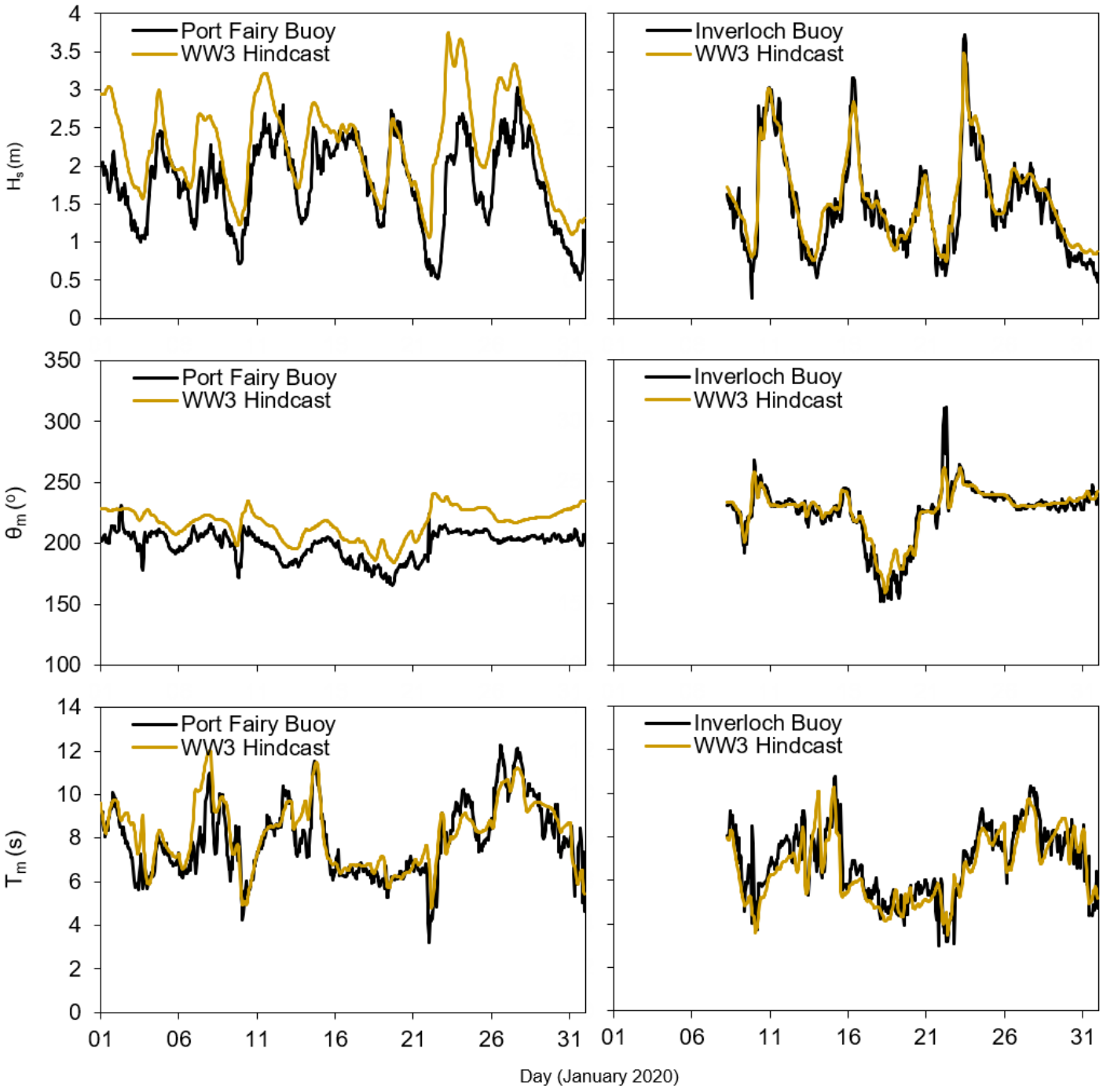

Figure 2

Comparison of significant wave height (Hs), mean wave period (Tm) and mean wave direction (θm) between modelled (WW3) and measured (buoy) data.

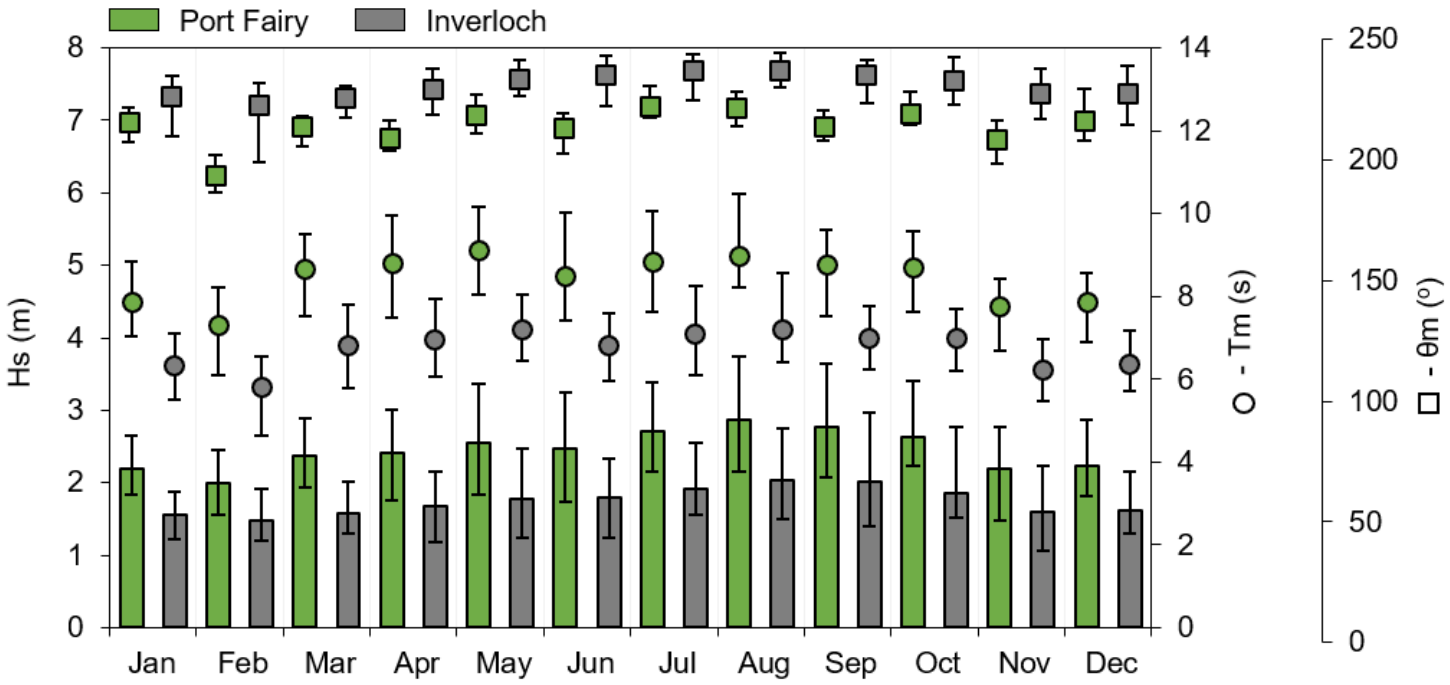

Figure 3

Wave climate seasonality derived from WW3 outputs between 1979-2020 in both Port Fairy (green) and Inverloch (grey). Hs is given in the bar chart, θm as squares and Tm as circles.

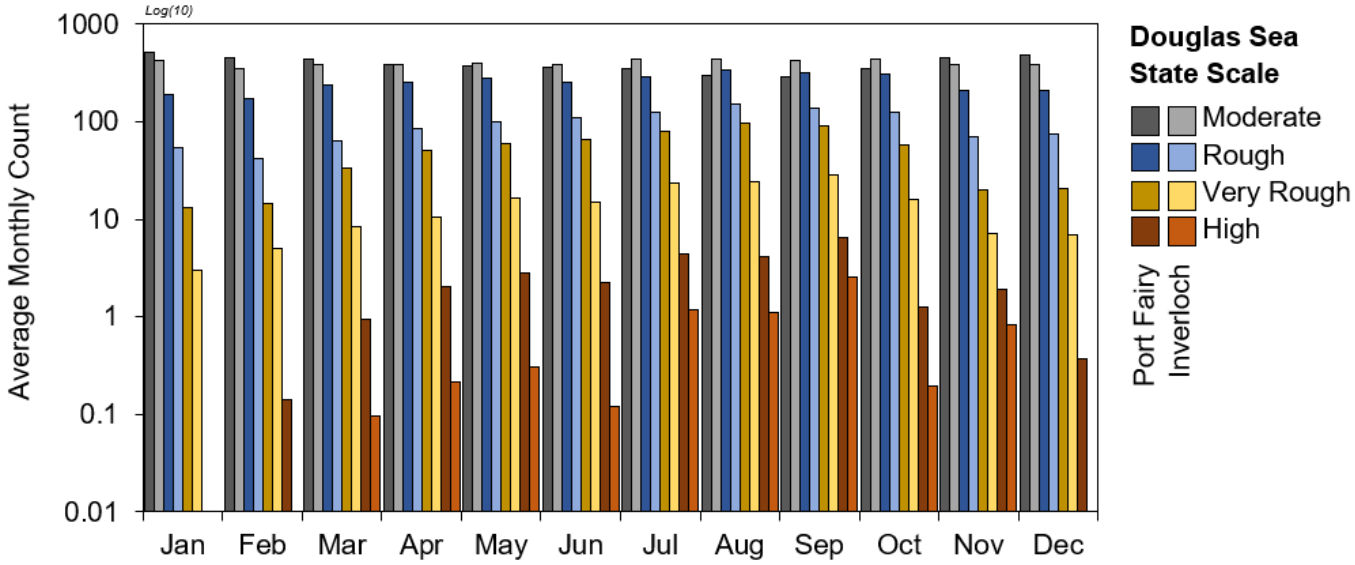

Figure 4

Average hourly exceedance per month (1979-2020) of moderate, rough, very rough and high sea states according to the Douglas Scale (Bureau of Meteorology 2020a), in Port Fairy and Inverloch.

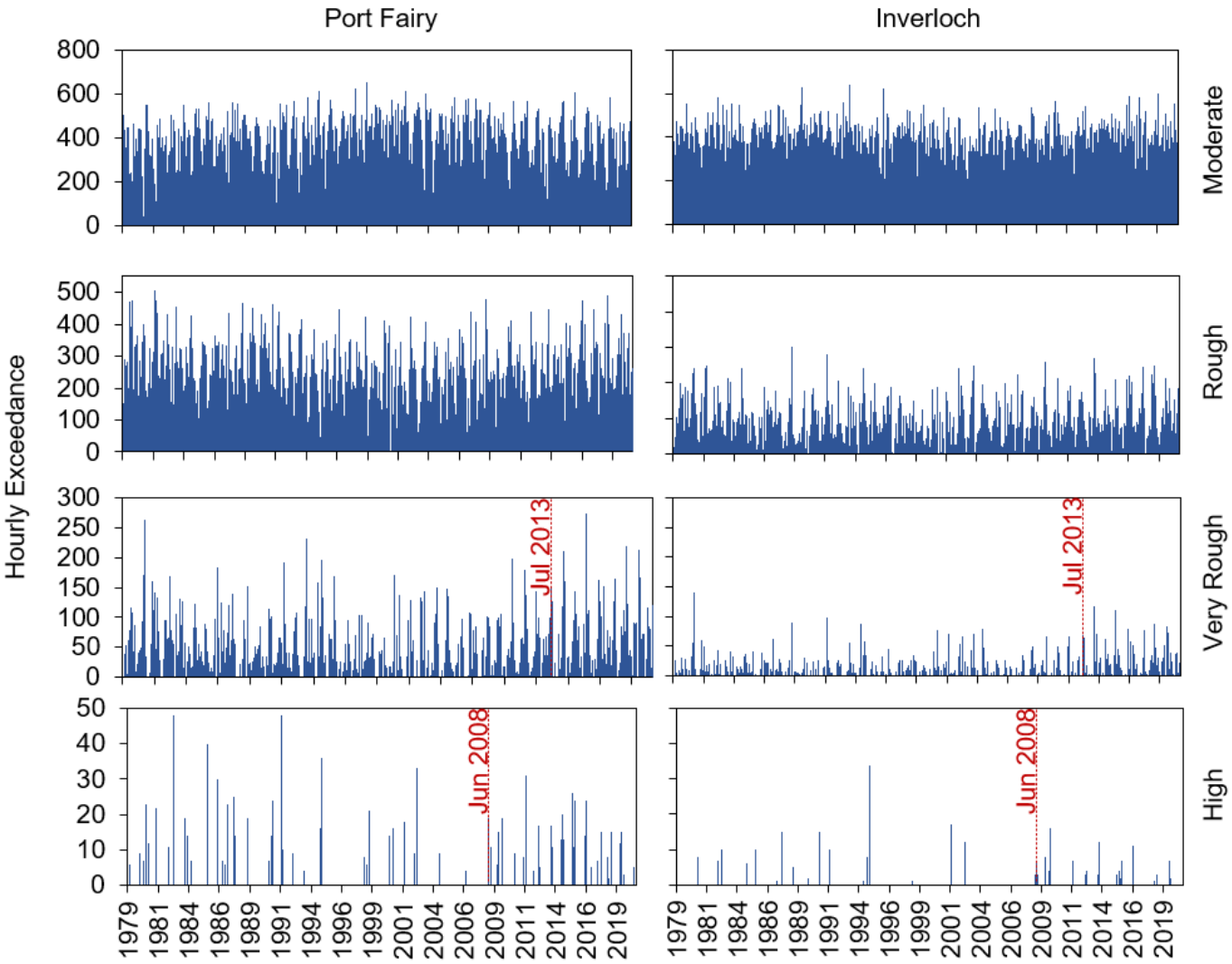

Figure 5

Hourly exceedance per month (1979-2020) for each sea state derived from WW3 outputs, for both Port Fairy and Inverloch. Periods identified as having a statistical increase in hourly exceedance of the given sea state are highlighted in July 2013 for 'Very Rough' sea states and June 2008 for 'High' sea states.

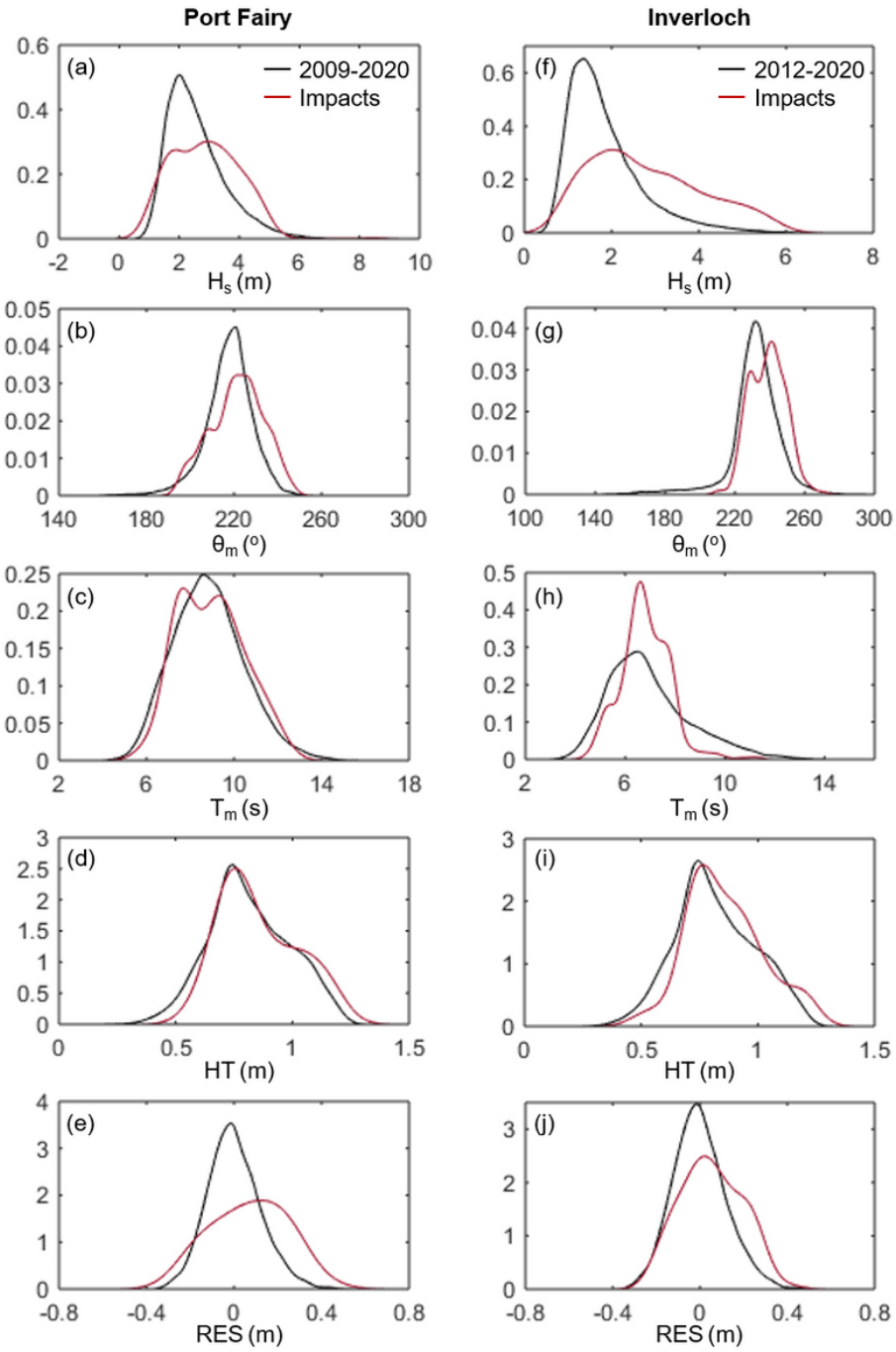

Figure 6

Kernel Density Estimates (KDE) for Hs (a,f), θm (b,g), Tm (c,h), HT (d,i) and RES (e,j), derived from hourly WW3 outputs for Port Fairy (left) and Inverloch (right). Black curves show KDE using all hours in the sample period (2009 – 2020 for Port Fairy, 2012-2020 for Inverloch), red curves show KDE derived using only for hours in sample period where coastal impacts were reported.

Supplementary Files

This is a list of supplementary files associated with this preprint. Click to download.

- ESM1.tif

- ESM2.tif
- OnlineResource1.png